SUPPLEMENTAL FIGURES and FIGURE LEGENDS

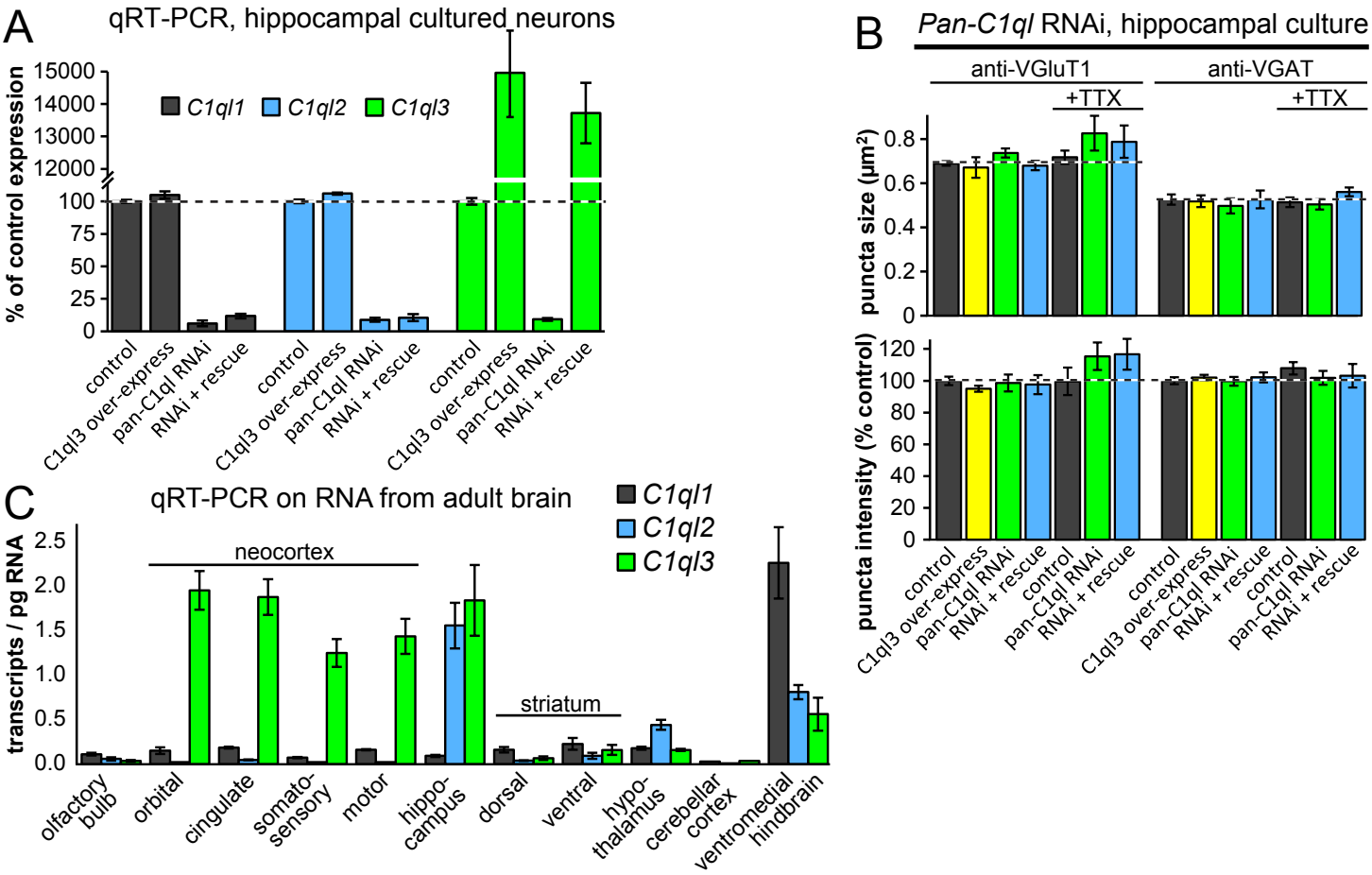

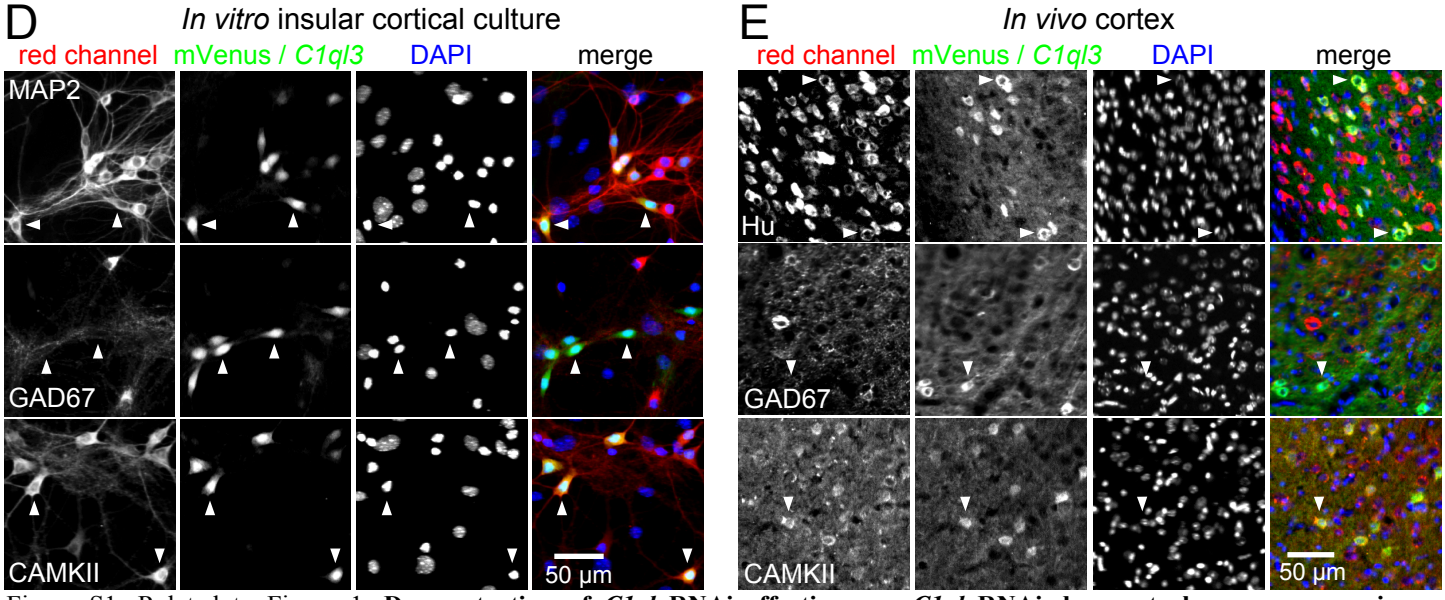

Figure S1. Related to Figure 1. **Demonstration of *C1ql* RNAi effectiveness; *C1ql* RNAi does not change synapse size or fluorescence intensity; *C1ql* family expression analysis in brain; and *C1ql3* expression in excitatory cortical neurons**

(**A**) qRT-PCR on DIV 14 hippocampal cultures after lentiviral-mediated *pan-C1ql* RNAi demonstrated reduction in each *C1ql* paralog and *C1ql3* overexpression/rescue with a *C1ql3* sequence modified to be impervious to the shRNA.

(**B**) Summary graphs of VGluT1 and VGAT puncta quantification in DIV 14 hippocampal cultured neurons after *pan-C1ql* RNAi, C1ql3 overexpression, or RNAi + C1ql3 rescue, ± TTX (for 3 days). Mean puncta area on top, mean indirect immunofluorescence signal intensity on bottom. Mean ± SEM.

(**C**) *C1ql* qRT-PCR on various dissected adult mouse brain regions. *C1ql4* values were so low that they were not visible, except in the hindbrain. Mean ± SEM; n = 3 mice.

(**D**) Double immunofluorescence for mVenus in *C1ql3*-expressing cells and neuronal markers in cultured cortical neurons. Arrowheads point to representative *C1ql3*-positive cells.

(**E**) Double immunofluorescence for mVenus in *C1ql3*-expressing cells and neuronal markers on adult mouse cryosections.

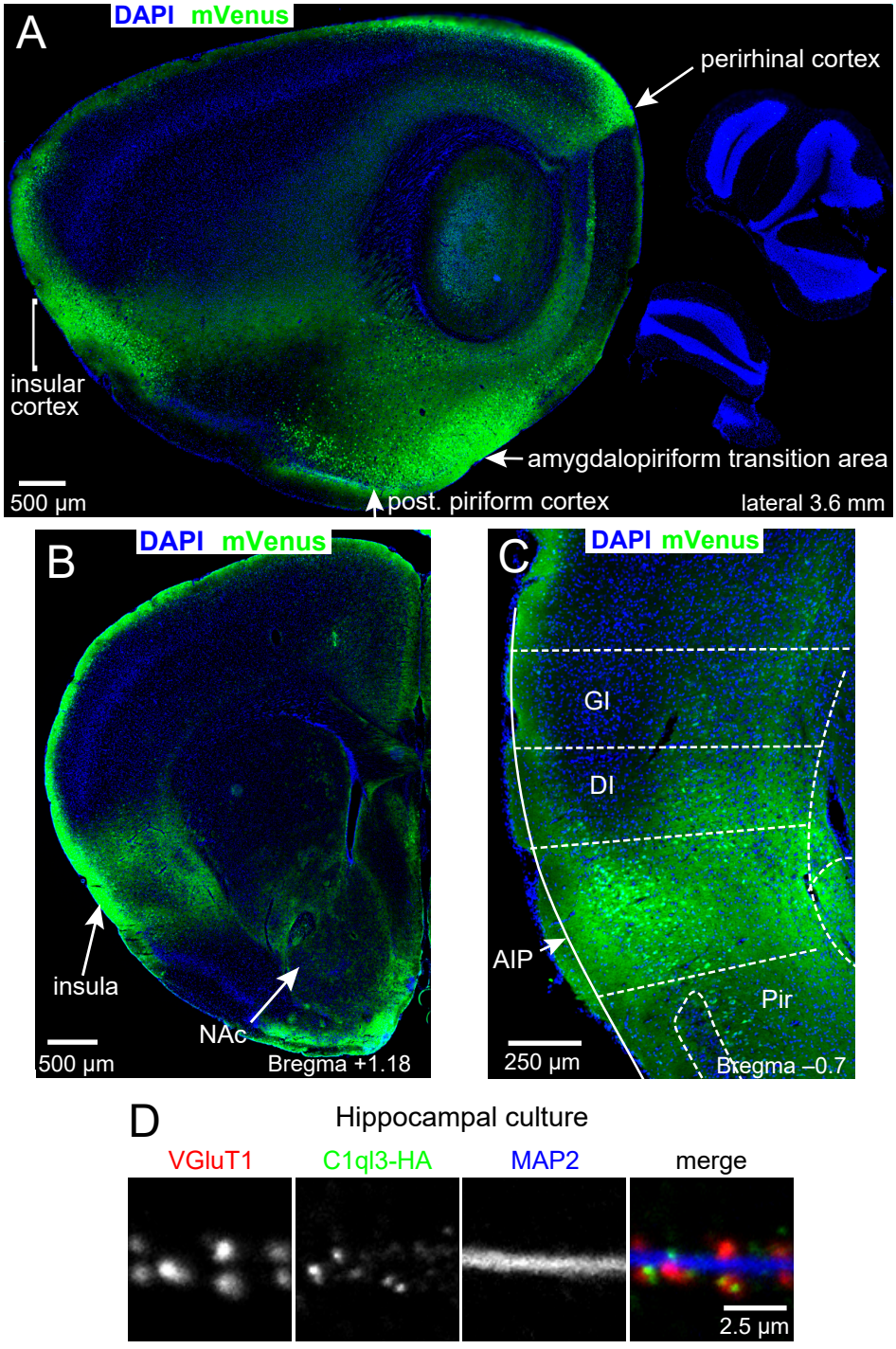

Figure S2. Related to Figure 2. **Additional immunofluorescence analyses of *C1ql3*-expressing neurons in adult brain using the knocked-in mVenus marker, and demonstration of the synaptic localization of C1ql3**

(**A–C**) Immunofluorescence for mVenus in *C1ql3*-expressing cells in adult brain in sagittal and coronal sections. AIP, posterior agranular insula; DI, dysgranular insula; GI, granular insula; NAc, nucleus accumbens; Pir, piriform cortex.

(**D**) Immunofluorescence for HA tag in hippocampal cultured neurons after lentivirus infection to express a C1ql3-HA protein. This revealed co-localization of C1ql3 with the presynaptic marker VGluT1.

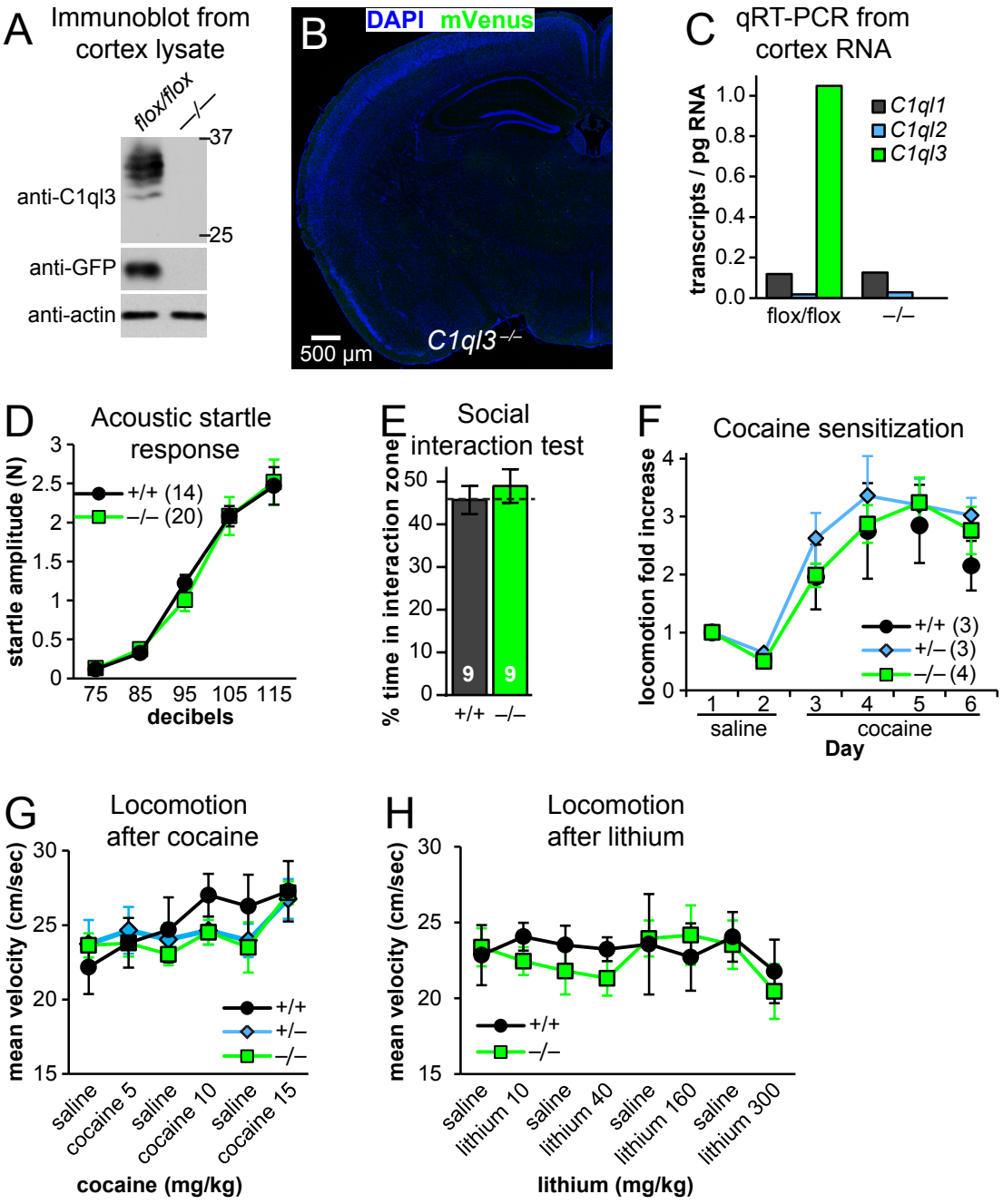

Figure S3. Related to Figure 3. **Confirmation of *C1ql3*$^{-}$ allele as null and additional behavior experiments on *C1ql3*$^{-/-}$ mice**

(**A**) Immunoblot for C1ql3 and mVenus demonstrating that Cre-mediated recombination creates a null-allele for *C1ql3* and silences mVenus expression. The second exon of the *C1ql3*^{flox} allele is floxed, which targets an essential part of the gC1q domain. An anti-GFP antibody recognized mVenus.

(**B**) Immunofluorescence for mVenus in a coronal section from a *C1ql3*$^{-/-}$ mouse brain demonstrating the absence of an mVenus signal.

(**C**) Measurements of *C1ql1*, *C1ql2*, and *C1ql3* mRNA levels by qRT-PCR on total RNA from adult cortex of *C1ql3* cKO (*C1ql3*$^{flox/flox}$) mice with or without Cre-recombinase mediated excision of *C1ql3* to demonstrate that the *C1ql3* deletion does not cause upregulation of *C1ql1* or *C1ql2*.

(**D**) Acoustic startle response at the indicated decibel levels.

(**E**) Social interaction test.

(**F**) In a distinct cohort of mice from the CPP experiment, *C1ql3*$^{-/-}$ mice had normal locomotor cocaine sensitization after consecutive days of cocaine administration (10 mg/kg).

(**G**) Locomotion data collected during the cocaine CPP experiment in figure 3J. There was no difference in movement velocity across the different genotypes.

(**H**) Locomotion data collected during the lithium CPA experiment in figure 3L. There was no difference in movement velocity across the different genotypes.

Mean ± SEM; n is depicted in graphs.

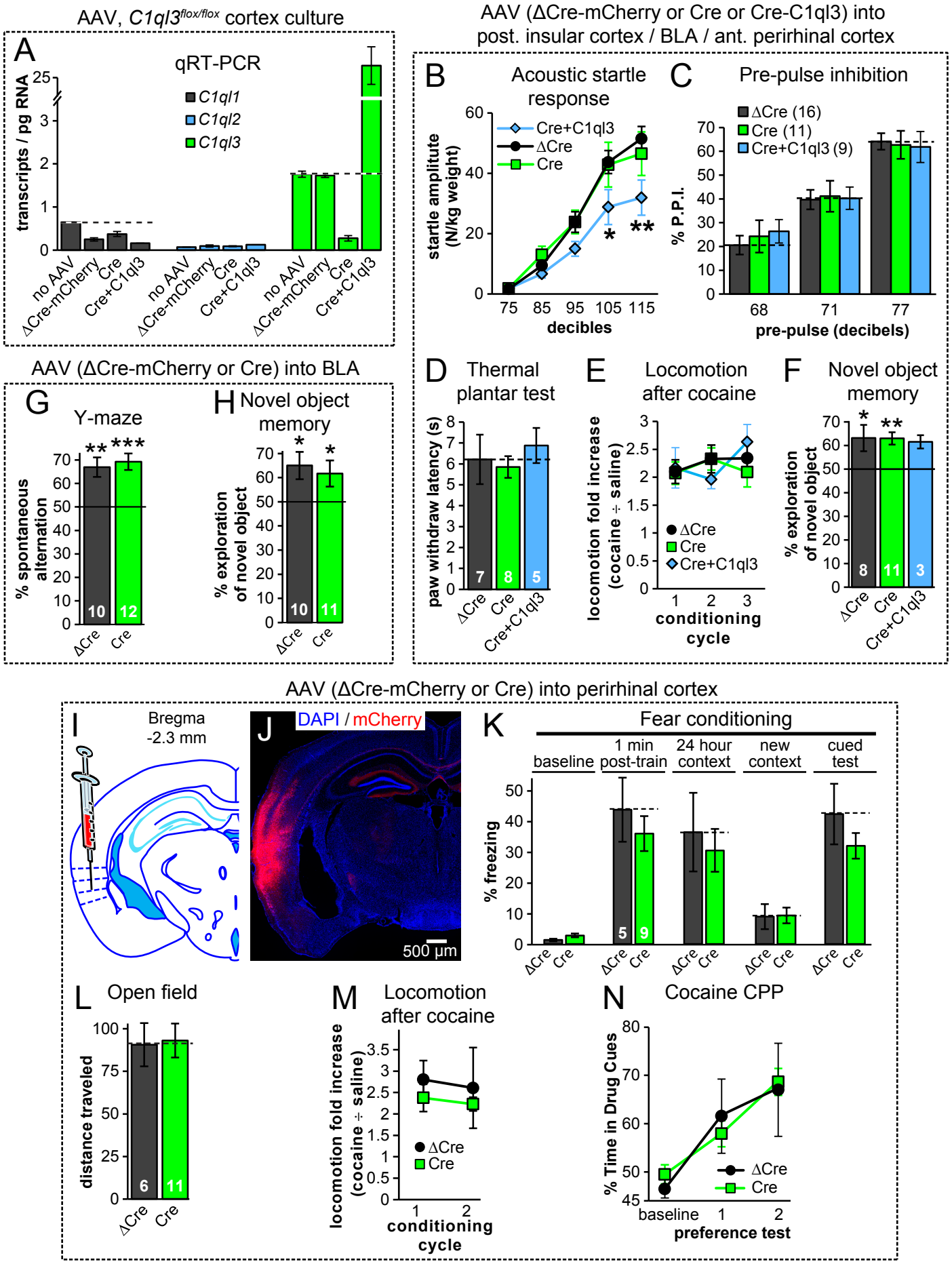

Figure S4. Related to Figure 4. **Additional experiments with *C1ql3* cKO mice after stereotactic injection of AAVs encoding ΔCre, Cre, Cre-IRES-C1ql3 to conditionally manipulate *C1ql3* expression in various brain regions.**

(**A**) qRT-PCR on DIV 14 cortical cultures from *C1ql3*$^{flox/flox}$ mice demonstrates effectiveness and specificity of AAV Cre vectors with or without C1ql3 overexpression as rescue.
(**B**) Effect of manipulations of *C1ql3* levels in acoustic startle response. Overexpression of C1ql3 caused a deficit for unknown reasons. Statistical significance was evaluated by repeated measures 2-way ANOVA with post-hoc Bonferroni's test.
(**C**) Pre-pulse inhibition of the acoustic startle response (115 decibel startle) at the indicated pre-pulse decibel levels.
(**D**) Thermal plantar test (Hargreaves' method) for pain sensitivity.
(**E**, **M**) Locomotion data collected during cocaine conditioned place preference experiments. 10 mg/kg dose was repeated for each conditioning cycle.
(**F**, **H**) 24 hour novel object recognition memory. Univariate t-test against 50%.
(**G**) Y-maze for percent spontaneous alternation (consecutive entry into each of the 3 arms in a Y-maze was scored for 5 min).
(**I**) Strategy for targeting AAV into perirhinal cortex.
(**J**) Representative cryosection of mCherry after AAV injection.
(**K**) Contextual and cued fear conditioning.
(**L**) 20 minute open field test.
(**N**) Cocaine-conditioned place preference. Dose of 10 mg/kg repeated for each conditioning cycle.
Mean ± SEM; n is depicted in graphs.

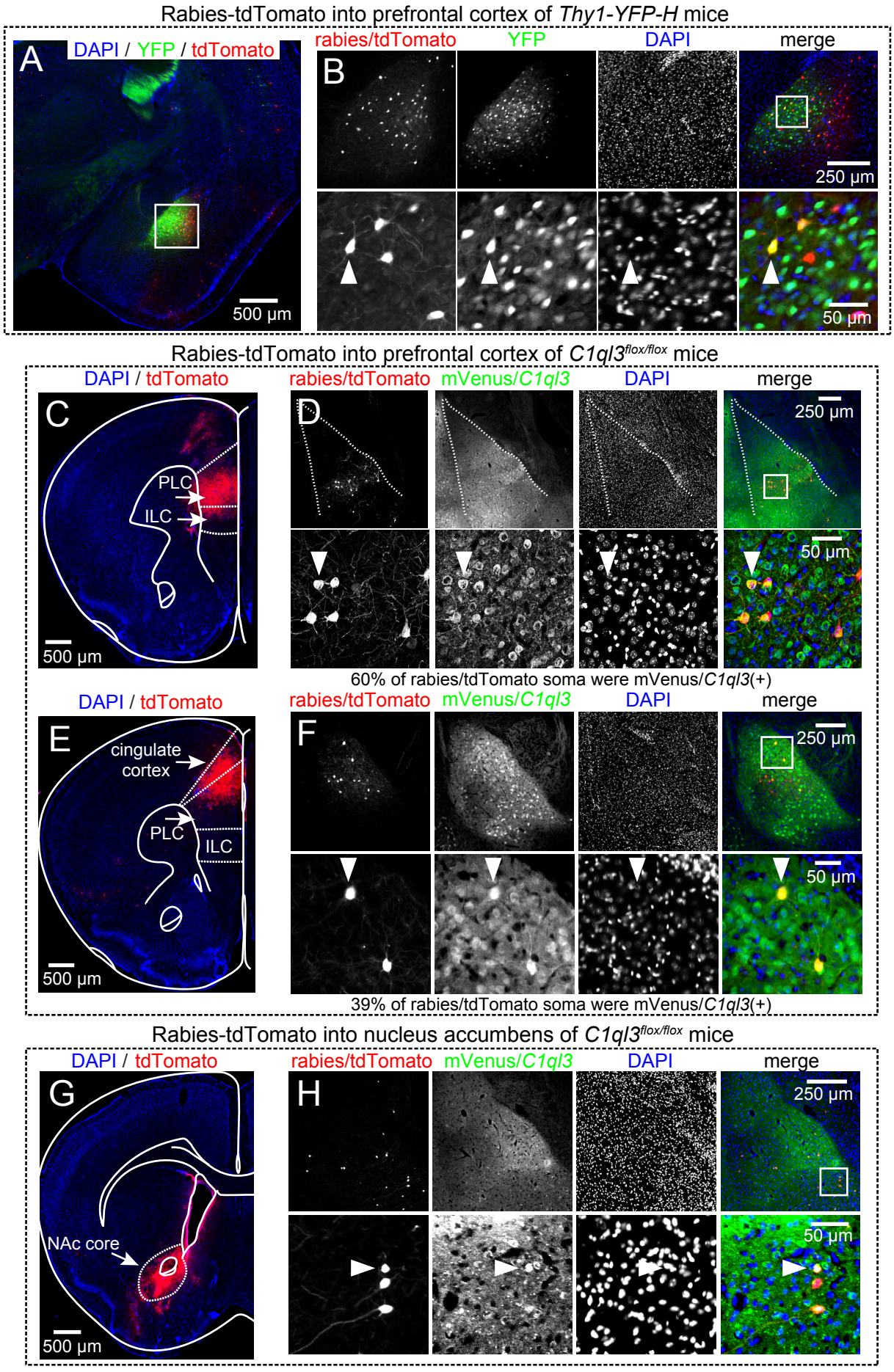

Figure S5. Related to Figure 5. ***Thy1-Yfp-H*** **expressing neurons in the BLA project to mPFC, and** ***C1ql3*****-expressing neurons in the BLA project to mPFC and the N. accumbens**

(**A**) Representative cryosection of tdTomato and YFP co-localization in BLA after rabies-tdTomato injected into mPFC of *Thy1-YFP-H* mice.
(**B**) Magnification of boxed region in panel A. Further enlargement in bottom row. Arrowhead indicates representative double positive soma.
(**C**, **E**, **G**) Representative cryosections of tdTomato after rabies injection into $C1ql3^{flox/flox}$ mice. PLC, prelimbic cortex; ILC, infralimbic cortex; NAc core, nucleus accumbens core.
(**D**, **F**, **H**) Representative cryosections of BLA from rabies virus injections, respectively. Magnification of boxed region in bottom row. Arrowhead indicates representative double positive soma.

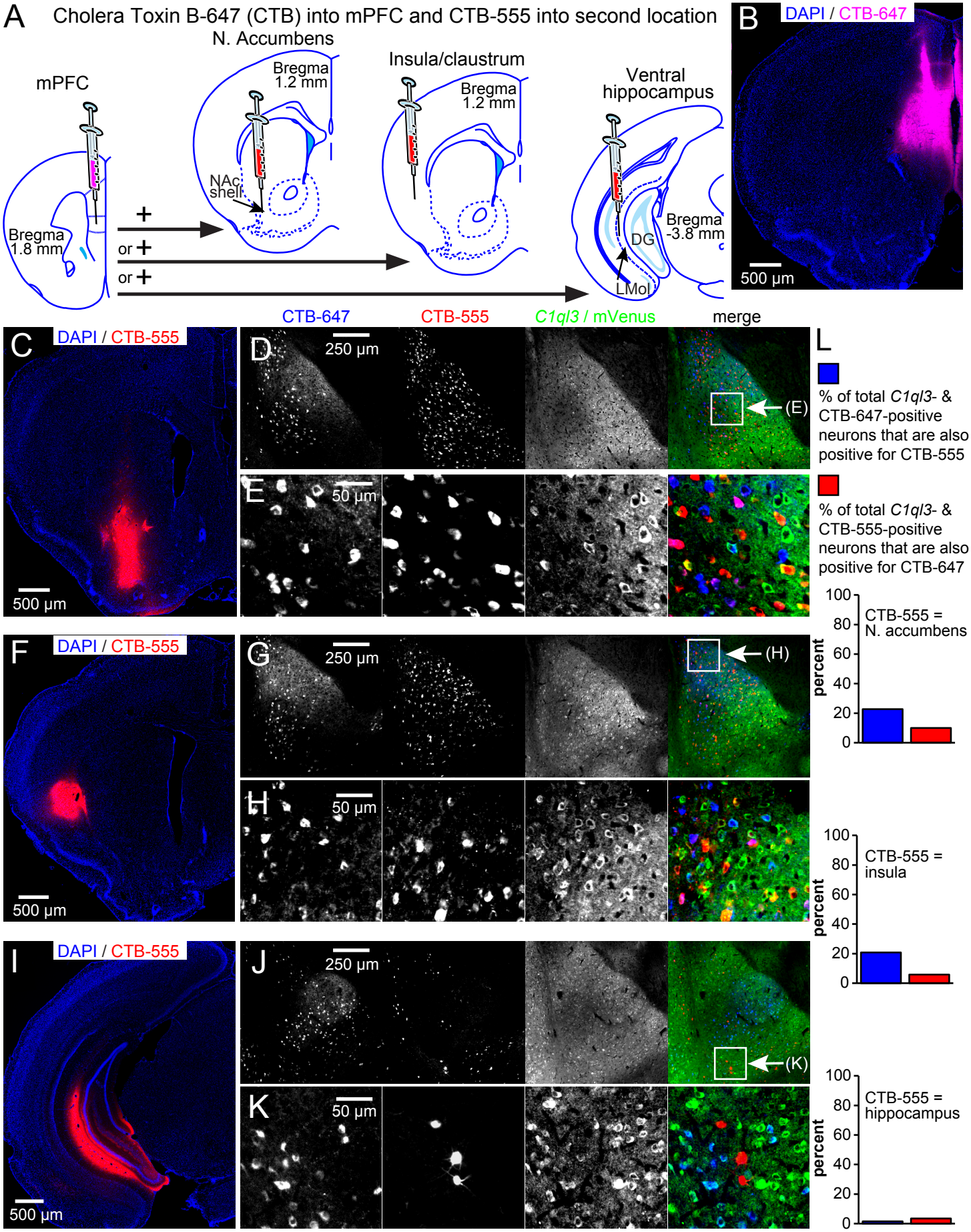

Figure S6. Related to Figure 6. ***C1ql3*-expressing BLA projection neurons mostly project to one location**

(**A**) Strategy for stereotactic injection of cholera toxin subunit B (CTB) conjugated to Alexa Fluor 647 into the mPFC of 9 week old *C1ql3*-mVenus knockin mice, and injection of CTB conjugated to Alexa Fluor 555 into three other brain areas as indicated. Each mouse received a similar CTB-647 injection into the mPFC, and then only one of the additional locations was targeted with CTB-555 for a total of two targeted locations per mouse. 6-8 days post-surgery, mice were perfused and cryosectioned. Injection sites were confirmed by fluorescence imaging, and the BLA was examined for co-localization of CTB-647 and CTB-555 along with mVenus, which marks *C1ql3*-expressing cells (abbreviations: DG, dentate gyrus. LMol, lacunosum moleculare layer of the hippocampus).
(**B**) Representative coronal section to illustrate CTB-647 targeting in the mPFC.
(**C**) Representative coronal section to illustrate CTB-555 targeting in the N. accumbens.
(**D**) Representative section to illustrate CTB-647, CTB-555, and mVenus localization in the BLA.
(**E**) Magnification of boxed BLA region in panel D.
(**F**–**K**) Similar to panels C–E, except CTB-555 was targeted to the insular cortex/claustrum or ventral hippocampus, respectively.
(**L**) Quantification of fluorescence co-localization in the BLA. Blue bars indicate the percent of cells that were double positive for *C1ql3*/mVenus and CTB-647 that were also positive for CTB-555, to measure the percent of *C1ql3*-positive mPFC projection neurons that also projected to an additional location. Red bars indicate the percent of cells that were double positive for *C1ql3*/mVenus and CTB-555 that were also positive for CTB-647, to measure the percent of *C1ql3*-positive N. accumbens, insula/claustrum, or hippocampus projection neurons that also projected to the mPFC.

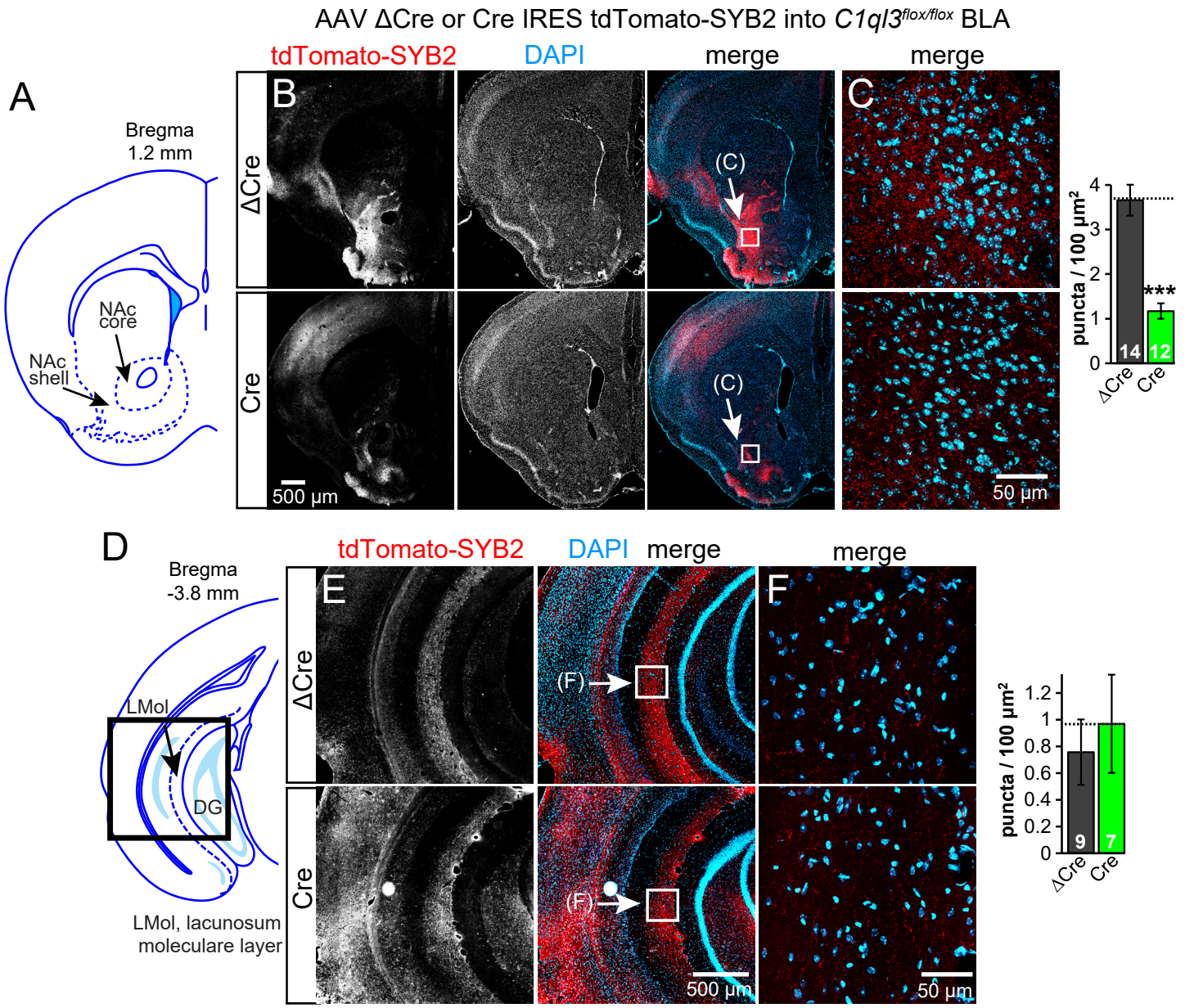

Figure S7. Related to Figure 7. **Conditional KO of *C1ql3* in the BLA decreases the density of synapses formed by BLA neurons projecting to the N. accumbens, but not to the ventral hippocampus**

(**A**) Diagram indicating the sub-divisions of the ventral striatum at the coronal section analyzed after anterograde labeling of synaptic projections using a modified SynaptoTag with tdTomato as a fluorophore. AAVs were injected into the BLA of 9 week old mice and analyzed 5 weeks later (NAc core, nucleus accumbens core; NAc shell, nucleus accumbens shell).

(**B**) Representative coronal sections illustrating that conditional KO of *C1ql3* in the BLA caused a large loss of presynaptic terminals projecting from the BLA to the nucleus accumbens. The densest projections were observed in the lateral shell region of the nucleus accumbens.

(**C**) Left, magnifications of the boxed regions in B. Right, summary graph of the density of synaptic puncta in the lateral shell of the nucleus accumbens.

(**D**) Diagram indicating the ventral hippocampal region analyzed after the ΔCre-IRES-tdTomato-SYB2 or Cre-IRES-tdTomato-SYB2 AAV were injected into the BLA. The most consistent projections observed were to the lacunosum moleculare layer of the ventral hippocampus.

(**E**) Representative coronal sections illustrating that conditional KO of *C1ql3* in the amygdala caused no loss of presynaptic terminals projecting to the ventral hippocampus. The red fluorescence signal was brightened compared to that of panel B.

(**F**) Left, magnifications of the boxed regions in E. Right, summary graph of the density of synaptic puncta in the lacunosum moleculare layer of the ventral hippocampus.

Data are means ± SEM; each AAV injected hemisphere was scored separately and the number of hemispheres analyzed is displayed in the graph. Statistical analyses were performed using Student's t-test.

SUPPLEMENTARY EXPERIMENTAL PROCEDURES

Neuronal culture experiments

All neurons were cultured onto glass coverslips coated with Matrigel from newborn mice as described (Bolliger et al., 2011). Hippocampal cultures were made from CD-1 mice. Cortical cultures were made from *C1ql3*$^{flox/flox}$ mice. The region of cortex cultured centered around the agranular insular and perirhinal cortices to enrich the fraction of plated neurons that were *C1ql3*-positive to ~50%, but generous amounts of adjacent cortex were also included. For lentivirus experiments, cultured neurons were infected on DIV 5 (250 µl / well) with freshly-made virus. For *in vitro* experiments with AAV, 0.1 µl (titer = 10^{10}/ml) of purified AAV was added to cultured neurons on DIV 8. Analysis on cultures was performed at DIV 14, except for figure 1C. For figure 1C, drugs were applied at DIV 14 and RNA harvested 3 days later. Concentrations of drugs used: TTX 1 µM, NBQX 10 µM, d-APV 50 µM (added fresh each day), picrotoxin 50 µM. For immunofluorescence, coverslips were fixed with cold methanol (-20°C) for 10 min. Images were acquired with a Nikon confocal microscope and Z-stacks were converted to maximal projections. For quantification of synaptic puncta, a novel program was coded for Mathmatica (Wolfram) to quantify synaptic puncta density, puncta surface area, and average puncta fluorescence intensity. Secondary dendrites on pyramidal-shaped neurons were photographed for quantification. Each experiment consisted of 3 coverslips per condition, and 15 dendritic segments analyzed per coverslip.

qRT-PCR

Total RNA was harvested from either freshly dissected brain pieces or from cultured neurons using the RNAqueous-Micro Kit (Ambion). PrimeTime qPCR assays were purchased from IDT and reactions were performed in a 7900 Fast Real-Time PCR machine (Applied Biosystems). For figure 1C, quantification was relative to the *Gapdh* reference assay. For figure S1C and S4A absolute quantification of transcript number was calculated with a standard curve method. Sequences used in this study are included in the following table:

mC1ql1	probe	TTTCACCTACCACGTCCTCATGCG
mC1ql1	reverse	CATAGTCGTAGTTCTGGTCTGC
mC1ql1	forward	CAACATTCCTGGCACCTACT
mC1ql2	probe	TGCCCGTTCTTGCAGAGATCCG
mC1ql2	reverse	TGCTGGCGTAGTCGTAATTC
mC1ql2	forward	ACGTACCACATTCTCATGCG
mC1ql3	probe	AGCATGTGGGCTGATCTCTGCAA
mC1ql3	reverse	GAAGGACCACACTGTTACTGG
mC1ql3	forward	CTACTTCTTCACCTACCACGTC

C1ql3 conditional mutant allele

The targeting vector was constructed using the recombineering technique as described in (Liu et al., 2003) and was electroporated into ES cells derived from F1 hybrid blastocyst of 129S6 x C57BL/6J. The G418 resistant ES clones were screened by nested PCR using primers outside the construct paired with primers inside the neo cassette. The sequences for primers used for ES cell screening were as follows: 5' arm forward primers: C1ql3 scr 5F1 (5'- gttccctggacaatgggcta) and C1ql3 scr 5F2 (5'- ggctacaaaggacatgactc). Reverse primers: frt scrR1 (5'- TTCTGAGGCGGAAAGAACCA) and frt scrR2 (5'- GGAACTTCATCAGTCAGGTA). 3' arm forward primers: mVenus scr 3F1 (5'- tgagctaccagtccaagctg) and mVenus scr 3F2, (5'- catggacgagctgtacaagt). Reverse primers: C1ql3 scr 3R1 (5'-AGAGTTTCCACTCTGGAGCT) and C1ql3 scr 3R2 (5'- AATGCCTGATGGCTTCCCAA). Chimeric mice were generated by aggregating ES cells with 8-cell embryos of CD-1 strain. The correct targeting was further confirmed by homozygosity testing. The neomycin resistance cassette was removed by breeding to mice expressing FLP recombinase (Dymecki, 1996) and the Flp transgene was bred out before experiments began. Mice harboring the novel allele were back-crossed to the C57BL6/J strain (C1ql3$^{tm1.1Sud}$ RRID: MGI_5779515). For genotyping, 3 primers in 1 reaction: C1ql3-F 5'TTCACATAGGTGCGTGCTAG, C1ql3-R 5'TAGCCATACGAATCCAGCGT, and mVenus-F 5'TGAGCTACCAGTCCAAGCTG. Mutant band = 244 bp, WT band = 187 bp.

Sequence of *C1ql3* conditional mutant allele

Sequence of the novel allele, beginning at the intron before first added loxp site:
atgaggctgaggcatagcttgaggaggggtggtggcagaatgtccataGGATCCACCTAATAACTTCGTATAGCATACATTATACGAAGTTATATTA
TGTACCTGACTGATGAAGTTCCTATACTTTCTAGAGAATAGGAACTTCGGAATTCgatatgcaatttgactgtttgcaaatgttgatcaaccctcta
atgaaacaaaggcagaacataagcagattatagtttgctcccatcctcaaagccagatacattgacaatctcataaaaaggaagagcaattcaacaataacctccagcaatcctagaaaactgtgcaa
tcttaggtcacacatttaatcccttctataacttttggatttggtgaacttaaatcgttgatttaaaggcattatataattatatgataaaaagacacaaaagaagtaaaaagaagtttgaaaatatgggagat
gcaaacaaatatgcttaagtgagtcacgctgtgtctgaagtagcctggataaaaggggctttgcatgtgtcagatttccaaagctttccaaaccgaaagctttctttctttatttttctctaggtcttttaccact
cgagatatgagatttctaataattaggatgacccattgaagtacacagttagtcgggatgctgttattTGATTTAAATTAAAATGCAAAACAATACTGCTATTTCCA
TTTCAAAATGTGACTGGATGTGGAGATTCGAGGAATCAGAAAAAGCAGCAATTGAAGAGAAAATTAGATTGGCATGCT

TTATTTACAAGGATAGAAAGGATGGCAGCAATGTCCCTTATTAAAGCAACATTTTTTTTCTCTTTTCTCTTTCCAGTAAC
ATAGTTGAAGTTGTTATGGAAATTCCTTCTAAACCTATGGGACCAACAGCAACATCAGTGTGCTACATTGTATGCTATG
GCTGCAAGTCTGCTATTATGTAAAAGGGGCAACTTAAGGATTCTCTATTTACAAACTAACTCTTGTCTGTTTCACATAGG
TGCGTGCTAGTGCAATTGCTCAAGATGCTGATCAGAATTACGACTATGCCAGTAACAGTGTGGTCCTTCACCTGGAACC
AGGAGATGAAGTCTATATCAAATTAGATGGTGGGAAAGCCCACGGAGGAAACAACAACAAATACAGCACATTCTCTGG
ATTTATTATTTATGCTGACTGATAATGCAGAGACTGATAACTTCGTATAGCATACATTATACGAAGTTATTTAATTAAGA
ATTCCgcccctctccctccccccccctaacgttactggccgaagccgcttggaataaggccggtgtgcgtttgtctatatgttattttccaccatattgccgtcttttggcaatgtgagggcccgga
aacctggccctgtcttcttgacgagcattcctaggggtctttcccctctcgccaaaggaatgcaaggtctgttgaatgtcgtgaaggaagcagttcctctggaagcttcttgaagacaaacaacgtctgt
agcgacccctttgcaggcagcggaacccccccacctggcgacaggtgcctctgcggccaaaagccacgtgtataagatacacctgcaaaggcggcacaaccccagtgccacgttgtgagttggata
gttgtggaaagagtcaaatggctctcctcaagcgtattcaacaaggggctgaaggatgcccagaaggtaccccattgtatgggatctgatctggggcctcggtgcacatgctttacatgtgtttagtcg
aggttaaaaaaacgtctaggccccccgaaccacggggacgtggttttcctttgaaaaacacgatgataatatggccacaaccatggtgagcaagggcgaggagctgttcaccggggtggtgccca
tcctggtcgagctggacggcgacgtaaacggccacaagttcagcgtgtccggcgagggcgagggcgatgccacctacggcaagctgaccctgaagctgatctgcaccaccggcaagctgccc
gtgccctggcccaccctcgtgaccaccctgggctacggcctgcagtgcttcgcccgctaccccgaccacatgaagcagcacgacttcttcaagtccgccatgcccgaaggctacgtccaggagcg
caccatcttcttcaaggacgacggcaactacaagacccgcgccgaggtgaagttcgagggcgacaccctggtgaaccgcatcgagctgaagggcatcgacttcaaggaggacggcaacatcct
ggggcacaagctggagtacaactacaacagccacaacgtctatatcaccgccgacaagcagaagaacggcatcaaggccaacttcaagatccgccacaacatcgaggacggcggcgtgcagc
tcgccgaccactaccagcagaacaccccccatcggcgacggccccgtgctgctgcccgacaaccactacctgagctaccagtccaagctgagcaaagaccccaacgagaagcgcgatcacatg
gtcctgctggagttcgtgaccgccgccgggatcactctcggcatggacgagctgtacaagtaatcctctagaGTCGAtcgaCCTCGAGGGCGCGCCTTGCTGTTCTGA
GTTT

Antibodies for immunofluorescence

The following antibodies were used in this study either on cryosections or cultured neurons: mouse anti-MAP2 (M1406 Sigma), mouse anti-GAD67 (Mab5406 Millipore), mouse anti-CAMKII (MAB 8699 Chemicon), mouse anti-HuC/HuD (Life Technologies A-21271), guinea pig anti-VGluT1 (AB5905 Millipore), rabbit anti-VGAT (131 003 Synaptic Systems), rabbit anti-C1ql3 (ab107006 Abcam), rabbit anti-HA (Sigma H6908), and mouse anti-flag (Sigma F3165). The anti-flag antibody was used to detect the flag epitope tag fused to Cre, which was only detectable after an antigen retrieval step consisting of 10 mM citrate, 0.05% Tween 20, pH 6.0 for 30 min at 95°C on free floating sections. The signal intensity of mVenus from the *C1ql3*^{flox} allele was low so an anti-GFP antibody was used to enhance signal; rabbit anti-GFP (A11122 Invitrogen). For the C1ql3 immunofluorescence, signal was only observed after pepsin treatment, as described in (Franciosi et al., 2007); although this treatment abolished the mVenus epitope. Secondary Alexa Fluor antibodies (Life Technologies) were used with appropriate fluorescent conjugates.

Behavior

All behavior experiments were performed on littermate male mice. The *C1ql3*^{flox} allele was converted to the *C1ql3*$^{-}$ allele by crossing to B6.C-Tg(CMV-cre)1Cgn/J mice. *C1ql3*$^{+/+}$, *C1ql3*$^{+/-}$, and *C1ql3*$^{-/-}$ (C1ql3$^{tm1.2Sud}$ RRID: MGI_5779517) mice were obtained by breeding *C1ql3*$^{+/-}$ mice. For the germline mutant analysis all mice were 2–3 months old. For virus injected mice, 3–5 months old.

Acoustic startle response and pre-pulse inhibition performed as described (Geyer and Dulawa, 2003) with apparatus built by Kinder Scientific and analyzed with Startle Monitor II software.

Rotating rod assay performed with apparatus and software from Med associates. 3 trials per day were conducted over 2 days for a total of 6 trials. The rotation speed of the rod started at 6 RPM and gradually accelerated to a maximum of 60 RPM. The rotation speed of the rod was recorded when the mouse fell. If a mouse stopped running and simply grasped the rod for a total of 3 revolutions, the trial was stopped and rotation speed recorded.

Open field performed using an actometer force plate for 20 min (Fowler et al., 2001).

Elevated plus maze performed as described (Walf and Frye, 2007) (except observation was for 10 min) and analyzed with Viewer^3 software from BIOBSERVE.

Fear conditioning performed using chamber built by Coulbourn Instruments and analyzed by FreezeFrame software. 2 min measurement of baseline activity in training chamber (mice were not pre-exposed to the chamber) followed by 5 training cycles each lasting 47 s and consisting of 15 s tone (90 dB volume) and 2 s foot shock (0.26 mA average intensity) co-terminating with the tone, 32 s inter-cycle interval. After last shock, 1 additional minute in the chamber. 1 day later mouse placed in training chamber and observed for 2 min. 2 days later mouse placed in an altered context chamber with vanilla scent and observed for 2 min to measure new baseline activity, followed by 1 min tone. For figure 4J, the conditional mutants were placed back into the altered context chamber 4 weeks post-training, and the day 3 protocol was repeated.

Cocaine or lithium place preference experiments adapted from (Cunningham et al., 2006) and see Figure 3I. In brief, the chamber floor was divided into a smooth-textured black half and a rough-textured white half designed to yield an 'unbiased' design in which the mice spend ~50% of the baseline session on each side. Each observation session was 20 min. After the first baseline test/habituation, the zone of the chamber to be paired with cocaine was randomly counter-balanced. Injections were administered IP and mice placed immediately into the chamber. Each conditioning cycle lasted 3 days and consisted of 1 day of drug, 1 day of saline (given in the opposite zone), and finally a preference test. Whether the drug (or saline) was given on the first (or second) day of the cycle was also counter-balanced. The number of conditioning cycles was 2, 3, or 4, depending on each experiment. The time spent in each zone was recorded using activity boxes made by Med Associates and analyzed by Activity Monitor software. Cocaine and lithium concentrations used are described in each figure legend.

Novel object recognition assay: Day 1, 20 min habituation in empty chamber. Day 2, 20 min in chamber with 2 identical objects, either 1 L bottle caps or blocks of Legos. Day 3, 1 object replaced with a novel object, and exploration scored for the first 20 seconds of total exploration time, or stopped at 10 min. Object location in chamber and objects given per genotype was counter-balanced. Exploration scored by hand with observer blinded to genotype.
Morris water maze performed as described (LeGates et al., 2012).
Social interaction test performed as described (Kaidanovich-Beilin et al., 2011) and analyzed with Viewer[3] software from BIOBSERVE.
Thermal plantar test performed as described (Hargreaves et al., 1988).
All mouse work was approved by animal use committees at Stanford University.

Virus vectors
All C1ql3 sequences are mouse. The following adeno-associated viruses (AAV-DJ) were used in this study, all with a synapsin promoter: ΔCre-P2A-mCherry, Cre-IRES-C1ql3-HA, Cre only, ΔCre-IRES-tdTomato-SYB2, Cre-IRES-tdTomato-SYB2, WGA-ΔCre-IRES-tdTomato, WGA-Cre-IRES-tdTomato, and Cre-IRES-tdTomato. All were sub-cloned from vectors from (Xu and Sudhof, 2013) and purified as described therein. P2A peptide derived from porcine teschovirus (Kim et al., 2011). The P2A peptide created 2 separated proteins. 2 nuclear localization signals were added to Cre. For the control vector (*i.e.* ΔCre), the Cre sequence was half-truncated creating a non-functional enzyme. A HA tag was added to the *C1ql3* sequences immediately after the signal peptide. For *C1ql* RNAi and rescue, the following lentiviruses were used: pL309 +shRNA#65, empty pL309 for control, pL309 +mCherry-IRES-C1ql3-HA, pL309 +shRNA#65 +mCherry-IRES-C1ql3-HA. All were sub-cloned from vectors described in (Pang et al., 2010). Sequence of shRNA: GGTTACGAGGTGCTCAAGTTT, designed to target *C1ql1–3*. *C1ql3* sequence modified to be less similar to the shRNA sequence. shRNA driven by H1 promoter. Protein expression driven by ubiquitin C promoter. All lentiviruses were produced as described (Maximov et al., 2009) except calcium phosphate was used for transfection of HEK293T cells. Calcium phosphate transfection resulted in ~10 fold higher titer compared to lipid based transfection reagents.
Rabies-tdTomato was generous gift from Robert Malenka's lab (Lim et al., 2012).

Stereotaxic virus or cholera toxin injection
All surgeries performed on littermate male mice 9 weeks old and 0.5 µl (titer = 10^{10}/ml) purified AAV injected per location at rate of 0.1 µl/min. All coordinates given as distance from bregma according to the mouse brain atlas (Paxinos and Franklin, 2004) and units in mm. For posterior insular cortex (which also infected the BLA), bilateral, A/P -0.7, D/V -2.9 with 6° angle, M/L ±3.45. For BLA (only 0.2 µl AAV per injection), bilateral: A/P -1.34, D/V -4.11 with 4° angle, M/L ±3.06. For perirhinal cortex, bilateral: A/P -2.3, D/V -2.5 with 7° angle, M/L ±3.95. For prefrontal cortex, bilateral: A/P +1.7, D/V -2.07 with 5° angle, M/L ±0.5. All experiments began 4 or 5 weeks after surgery, as noted in text.
For rabies virus into prefrontal cortex, injection was unilateral and mice were perfused 3-4 days after injections.
For cholera toxin subunit B (CTB) injections, two were purchased from ThermoFisher Scientific: an Alexa Fluor 555 conjugate and a 647 conjugate. The CTB-647 was bilaterally injected into the mPFC and the CTB-555 was bilaterally injected into the nucleus accumbens shell, insular cortex, or the ventral hippocampus of the same mouse. Mice were perfused 6 – 8 days later to examine for co-localization of the two fluorophores in the BLA.

Electron Microscopy
Brain tissue from littermate wild-type and mutant (constitutive *C1ql3* KO) mice were embedded in epon resin (Electron Microscopy Science, EMS, Hatfield, USA). For embedding, anesthetized mice (3-5 months) were transcardially perfused with 30 ml of 2% glutaraldehyde and 2% paraformaldehyde in 0.1 M PB and postfixed at 4°C overnight. Blocks of prefrontal cortical tissue were contrasted in 1% OsO_4 for 2 hours at RT. Following washes with dH_2O and dehydrating, tissue was incubated with propylene oxide for 45 min, infiltrated with propylene oxide/epon (1:1) for 1 hour, in pure epon overnight, and hardened at 60°C for 24 hrs. Contrasting of thin sections from brains was done on Formvar and carbon-coated copper grids with a solution of 3.5% uranyl acetate and lead citrate.
For ultrastructural analysis, samples were investigated with a transmission electron microscope at 120 kV (JOEL JEM1400, Stanford Microscopy Facility), and images taken with a CCD camera (GatanMicroscopy Software). For morphometry, images from Epon-embedded medial prefrontal cortex (mPFC) of each animal were examined at 5,000x primary magnification. An observer blinded to the genotype of the sample took a series of images at the border of layer 1 to 2 of the prelimbic cortex. Asymmetric (type 1) synapses were defined as contacts with a visible synaptic cleft, a distinct postsynaptic density and at least three synaptic vesicles. In perforated type 1 synapses, the postsynaptic density was classified as discontinuous. Total asymmetric synapses and perforated synapses were quantified as area densities by an observer blinded to the genotype of the sample, and the ratio of perforated to non-perforated synapses was calculated. Length of postsynaptic densities was determined by a straight line between its outer borders. Symmetric synapses were observed in both genotypes, appeared grossly anatomically normal, but were not quantified due to low density in this area. For additional parameter measurements, images were analyzed at primary magnification of 10,000x, and include 20-23 asymmetric, non-perforated synapses per animal (N = 61 synapses/ WT; and N = 73 synapses/ KO) with perpendicularly cut synaptic cleft from the layer 1/2 transition zone.

SUPPLEMENTARY REFERENCES

Bolliger, M.F., Martinelli, D.C., and Sudhof, T.C. (2011). The cell-adhesion G protein-coupled receptor BAI3 is a high-affinity receptor for C1q-like proteins. Proc Natl Acad Sci U S A *108*, 2534-2539.

Cunningham, C.L., Gremel, C.M., and Groblewski, P.A. (2006). Drug-induced conditioned place preference and aversion in mice. Nature protocols *1*, 1662-1670.

Dymecki, S.M. (1996). Flp recombinase promotes site-specific DNA recombination in embryonic stem cells and transgenic mice. Proc Natl Acad Sci U S A *93*, 6191-6196.

Fowler, S.C., Birkestrand, B.R., Chen, R., Moss, S.J., Vorontsova, E., Wang, G., and Zarcone, T.J. (2001). A force-plate actometer for quantitating rodent behaviors: illustrative data on locomotion, rotation, spatial patterning, stereotypies, and tremor. Journal of neuroscience methods *107*, 107-124.

Franciosi, S., De Gasperi, R., Dickstein, D.L., English, D.F., Rocher, A.B., Janssen, W.G., Christoffel, D., Sosa, M.A., Hof, P.R., Buxbaum, J.D., *et al.* (2007). Pepsin pretreatment allows collagen IV immunostaining of blood vessels in adult mouse brain. Journal of neuroscience methods *163*, 76-82.

Geyer, M.A., and Dulawa, S.C. (2003). Assessment of murine startle reactivity, prepulse inhibition, and habituation. Current protocols in neuroscience / editorial board, Jacqueline N Crawley [et al] *Chapter 8*, Unit 8 17.

Hargreaves, K., Dubner, R., Brown, F., Flores, C., and Joris, J. (1988). A new and sensitive method for measuring thermal nociception in cutaneous hyperalgesia. Pain *32*, 77-88.

Kaidanovich-Beilin, O., Lipina, T., Vukobradovic, I., Roder, J., and Woodgett, J.R. (2011). Assessment of social interaction behaviors. Journal of visualized experiments : JoVE.

Kim, J.H., Lee, S.R., Li, L.H., Park, H.J., Park, J.H., Lee, K.Y., Kim, M.K., Shin, B.A., and Choi, S.Y. (2011). High cleavage efficiency of a 2A peptide derived from porcine teschovirus-1 in human cell lines, zebrafish and mice. PloS one *6*, e18556.

LeGates, T.A., Altimus, C.M., Wang, H., Lee, H.K., Yang, S., Zhao, H., Kirkwood, A., Weber, E.T., and Hattar, S. (2012). Aberrant light directly impairs mood and learning through melanopsin-expressing neurons. Nature *491*, 594-598.

Lim, B.K., Huang, K.W., Grueter, B.A., Rothwell, P.E., and Malenka, R.C. (2012). Anhedonia requires MC4R-mediated synaptic adaptations in nucleus accumbens. Nature *487*, 183-189.

Liu, P., Jenkins, N.A., and Copeland, N.G. (2003). A highly efficient recombineering-based method for generating conditional knockout mutations. Genome research *13*, 476-484.

Maximov, A., Tang, J., Yang, X., Pang, Z.P., and Sudhof, T.C. (2009). Complexin controls the force transfer from SNARE complexes to membranes in fusion. Science *323*, 516-521.

Pang, Z.P., Cao, P., Xu, W., and Sudhof, T.C. (2010). Calmodulin controls synaptic strength via presynaptic activation of calmodulin kinase II. J Neurosci *30*, 4132-4142.

Paxinos, G., and Franklin, K.B.J. (2004). The mouse brain in stereotaxic coordinates, Compact 2nd edn (Amsterdam ; Boston: Elsevier Academic Press).

Walf, A.A., and Frye, C.A. (2007). The use of the elevated plus maze as an assay of anxiety-related behavior in rodents. Nature protocols *2*, 322-328.

Xu, W., and Sudhof, T.C. (2013). A neural circuit for memory specificity and generalization. Science *339*, 1290-1295.